LBL-34181
UC-405
Preprint

Lawrence Berkeley Laboratory

UNIVERSITY OF CALIFORNIA

Physics Division

Mathematics Department

Submitted for publication

Vortex Solids and Vortex Liquids in a Complex Ginzburg-Landau System

G. Huber

May 1993

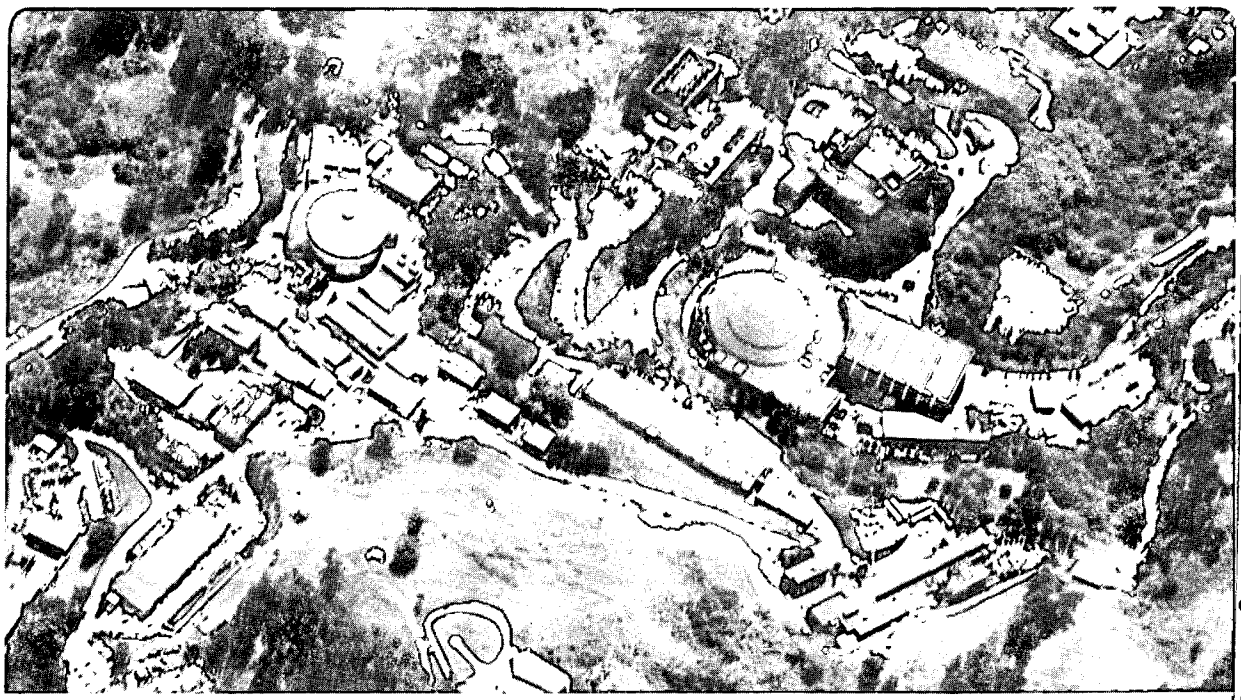

REFERENCE COPY
Does Not
Circulate
Bldg. 50 Library.
LBL-34181
Copy 1

Prepared for the U.S. Department of Energy under Contract Number DE-AC03-76SF00098

DISCLAIMER

This document was prepared as an account of work sponsored by the United States Government. While this document is believed to contain correct information, neither the United States Government nor any agency thereof, nor the Regents of the University of California, nor any of their employees, makes any warranty, express or implied, or assumes any legal responsibility for the accuracy, completeness, or usefulness of any information, apparatus, product, or process disclosed, or represents that its use would not infringe privately owned rights. Reference herein to any specific commercial product, process, or service by its trade name, trademark, manufacturer, or otherwise, does not necessarily constitute or imply its endorsement, recommendation, or favoring by the United States Government or any agency thereof, or the Regents of the University of California. The views and opinions of authors expressed herein do not necessarily state or reflect those of the United States Government or any agency thereof or the Regents of the University of California.

LBL-34181

VORTEX SOLIDS AND VORTEX LIQUIDS IN A COMPLEX GINZBURG-LANDAU SYSTEM[1]

Greg Huber

Lawrence Berkeley Laboratory
and
Department of Mathematics and Department of Physics
University of California
Berkeley, CA 94720

May 1993

[1] This work was supported in part by the Applied Mathematical Sciences Subprogram of the Office of Energy Research, U.S. Department of Energy under Contract DE-AC03-76SF00098.

20 May 1993

Vortex solids and vortex liquids in a complex Ginzburg-Landau system

Greg Huber

Lawrence Berkeley Laboratory, and Department of Mathematics

and Department of Physics, University of California, Berkeley, California 94720 USA

1. Introduction

Order and disorder in oscillatory media are closely connected with the presence of topological defects. In a large class of two-dimensional chemical, optical and hydrodynamic systems, the dynamics is dominated by point defects (or vortices) and the extended spiral wave patterns they can generate. The goal in this paper is to present some of the phenomena seen in large-scale, parallel computer experiments. For this, a discrete form of the complex Ginzburg-Landau (CGL) equation based on a coupled-map lattice[11] is used to explore the defect dynamics. This algorithm defines a new Ginzburg-Landau system, but one whose properties can be brought into arbitrarily close correspondence with those of the complex Ginzburg-Landau equation. Details of this particular construction have appeared elsewhere.[2,3]

2. The CGL equation

The prototype for modeling defect dynamics in oscillatory media is the complex Ginzburg-Landau equation,

$$\dot{A}(\mathbf{x},t) = A(\mathbf{x},t) - (1+i\alpha)|A(\mathbf{x},t)|^2 A(\mathbf{x},t) + (1+i\beta)\nabla^2 A(\mathbf{x},t), \tag{1}$$

which describes the behavior of a slowly-varying complex amplitude field $A(\mathbf{x},t)$ in the neighborhood of a Hopf bifurcation.[9,10] The parameters α and β are real numbers, and one

research goal is to map out the asymptotic solutions in an α-β phase diagram (Figure 1).[1,7] The global, homogeneous solution $A(t) = \exp(-i\alpha t)$ is linearly stable when the condition $\alpha\beta + 1 > 0$ is satisfied (the Benjamin-Feir condition). This result can be reproduced in the coupled-map formalism, but due to our choice of discrete time steps, the analogous stability condition is $\alpha\beta + \gamma > 0$, where $\gamma = 0.824$. This stability limit is labeled "BF" in Figure 1.

3. Vortex phases

Qualitatively different from the homogeneous state, are solutions that allow the field A to assume phase-less points. In the two-dimensional context, these defects are referred to as *vortices*, since the phase undergoes a complete rotation on a closed loop encircling one. If the loop direction and induced phase rotation have the same sense, then the defect is properly called a vortex; if opposite senses, then an *antivortex*. Viewed as topological excitations, the vortices and antivortices carry positive and negative *topological charge*, respectively. (Where the distinction between vortices and antivortices is irrelevant, we refer to them collectively as vortices.) At the phase singularity, $|A| = 0$. Amplitude portraits clearly show the vortices as amplitude minima; also, one-dimensional structures (*domain walls*) corresponding to amplitude maxima are found separating the vortices.

If the initial conditions are random (this and periodic boundary conditions apply to all the simulations described here), the subsequent evolution in some cases does resemble the relaxation of a thermodynamic system following a deep quench.[6] In general, however, the system does *not* settle, even at very long times, into the homogeneous state; rather it finds a many-vortex state. This can be either a "frozen" (or "solid") state of stationary vortices, or a turbulent ("liquid") state[5] characterized by a high density of vortices, and vortex-antivortex creation and annihilation. In the α-β diagram of Figure 1, the curve $\alpha_0(\beta)$ marking the transition from frozen to turbulent states (labeled "T") was found point by point, by fixing β and carefully charting the time history of the total vortex number at various α values. In a paper with Alstrøm and Bohr[7], this transition was found to have

many properties of a first-order phase transition. Furthermore, plots of vortex density versus time provide a tool for directly tracing the different dynamical regimes. As an example representing the variety of dynamical changes, consider the log-log density trace in Figure 2. Four distinct dynamical behaviors can be identified: initial decay, transient turbulence, decay to frozen state ("Zamboni clean-up"), and frozen state. This is the generic dynamics in the parameter region lying between the curves T and NUC (Figure 1), this latter curve marking the appearance of transient turbulence and subsequent nucleation phenomena. (By comparison, the boundary of the Eckhaus instability (ECK), that is associated with the observed spiral waves states, lies somewhat lower in the α-β diagram. The gap between these curves is not completely understood.[1,7])

4. Nucleation and growth

We consider first the vicinity of the "knee" in Figure 2. It is helpful to see the system as it decays out of the turbulent transient, as in Figure 3 (a) - (c). (These are actually taken from three different runs, at three successive times, using the same parameter values.) The phenomenon observed in these amplitude portraits is the nucleation and growth of spiral waves. (In fact, the spiral waves can only be seen in the corresponding phase portrait.) These *vortex droplets* nucleate out of the turbulent sea, and grow until the entire space is covered by the frozen phase. Here the turbulent state is unstable with respect to the finite-sized droplets; in other words, the transient state can be viewed as a *metastable* state. It was found[7] that the average lifetime T of the metastable state is dependent on the distance to the turbulence transition line $\Delta\alpha$ $(= \alpha_0(\beta) - \alpha)$ according to the simple law,

$$T \sim e^{\mathrm{const}/(\Delta\alpha)^2}. \tag{2}$$

The divergence of the lifetime is one means of locating the transition curve $\alpha_0(\beta)$.

The relatively rapid decay of the vortex density toward the frozen density is due to the steady growth of the vortex droplets at the expense of the turbulent fraction, labeled

the "Zamboni clean-up"[12] in Figure 2. There is a general decay law lurking in that figure, but it is hidden by the log-log axes. Plotting the same regime for two different α values makes clear the parabolic nature of the decay in density (Figure 4). A model consisting of circular regions with radii growing linearly in time, together with a few other reasonable assumptions, leads to a density decreasing like $-t^2$, and accounts for the parabola law.

5. Vortex solid: domain walls, polycrystals, edge vortices

The amorphous frozen state seen in Figure 3 (c) is a fascinating structure, about which little is known. The subtle degrees of order and disorder evident here are a topic of on-going research. Note that some information on the vortex state is absent from the amplitude picture in Figure 3. The relative phase and direction of the spiral waves cannot easily be read off the picture. The vortex cells are typically evolving toward four or five-sided polygons, distinctly different from the Voronoi polygons calculated from the vortex centers. For starters, the domain walls are not straight line segments, but show various curvatures. Their numerical shape is well approximated by a hyperbola. This can be understood from a simple argument based on the nucleation picture. Let Δt_0 be the interval of time between the nucleation of two neighboring vortex droplets. Then, considering the two frozen vortices as the sources of two annihilating, nearly-plane waves (the spiral waves), the interface between them can be described by the radial path difference from the two vortex cores $r_1 - r_2$ (Figure 5). We have the usual relation,

$$r_1 - r_2 = \frac{2\pi\omega}{q}\Delta t_0. \tag{3}$$

Since Δt_0 is fixed, and the vortices have the same values of q and ω, the right-hand side of Eq. (3) is constant – this is just the equation for a hyperbola. Only when all the vortices nucleate at the same time ($\Delta t_0 = 0$), do we come back to the Voronoi picture of straight, bisecting domain walls.

Although the positions of the vortex centers are disordered, the field A within a vortex cell can be thought of as perfect spiral wave, like a spatiotemporal crystal. In fact, the

array of polygonal vortex cells strongly resembles the microstructure of polycrystalline materials. We illustrate this point in Figure 6 with two diverse examples. Figure 6 (a) is a scanning-tunneling micrograph of the grain structure of hot-pressed alumina; Figure 6 (b) a photograph of spherulites of low-density polyethylene grown from a thin-film melt, and viewed in polarized light (hence the Maltese-cross pattern). And these cellular arrays of metallic grains, or of polymer spherulites, are not isolated examples – polycrystals are a common structural motif in nature. The analog of the disorder in relative phase of the spirals is present as the random orientation of the crystal axes within a grain.

Analogies to the formation and growth of polycrystalline patterns are likewise intriguing. The spherulite example shows striking parallels. Nucleation and growth of spherulites is the characteristic mode of polymer crystallization from the melt, and the parabola law is found there as well.[8] Moreover, it is interesting to note that the helically-varying orientation of the crystal creates a tightly-wound spiral pattern in polarized light. This makes photographs of nucleating spherulites eerily reminiscent of nucleating spiral waves.[4,8]

The existence of *edge* vortices, which do not generate extended spiral waves, is another suprise revealed by the simulations. In a sense, they control the dynamics of an otherwise frozen set of vortex cells. They move along the domain walls, braiding the walls roughly one wavelength around them, only coming to rest at the intersection of two domain walls. In doing so, they act somewhat like zippers, "unzipping" or changing the phase to new value along the domain wall. As they diffuse around the network of domain walls, their numbers decrease due to vortex-antivortex annihilations at the interstices. A number of long-lived edge-vortex arrangements have been observed in the simulations. A common configuration is a bound vortex-antivortex pair. Triplets, quadruplets and higher-order combinations are also seen. One beautiful configuration of same-sign edge vortices is the *vortex braid.* Figure 7 is a schematic of a vortex braid, really an antivortex braid, redrawn from an amplitude portrait. Positively-charged vortex braids resemble the mirror of this drawing.

6. Questions

To conclude, we present some unanswered questions. The presumed glass-like order of the vortex positions motivates one to look for a *bona fide* glass transition. Is there a vortex solid with a density just slightly less than the high liquid density? And is there an associated second-order transition to the vortex-liquid phase? Since the metastability (NUC) and turbulent transition (T) lines seem to meet somewhere near the $\beta = 0$ axis, future work in this region of the phase diagram is called for.

Are the vortex solids described here "frozen"; that is, truly asymptotic states, or are they metastable, finally relaxing to a single vortex-antivortex pair, independent of system size? The present simulations show no trend toward such a zero-density state, however the possibility of dynamics on geological time scales cannot be eliminated. The addition of an explicit noise term to Eq. (1) would be step towards settling this issue.

Finally, the analogous vortex-line phases in three dimensions are completely unexplored. We end with a teaser in the form of Figure 8. It shows two sets of amplitude isosurfaces, one corresponding to vortex filaments, the other to domain walls. At the top of the cube, a two-dimensional slice shaded by amplitude shows off some of the filaments threading through the volume.

Acknowledgements

Discussions with P. Alstrøm, T. Bohr, L. Kramer, and S. Strogatz are gratefully acknowledged. This work is supported by the Applied Mathematical Sciences Subprogram of the Office of Energy Research, U. S. Department of Energy under Contract DE-AC03-76SF00098.

References

1. Aranson, I. S., Aranson, L. B., Kramer, L., and A. Weber. *Phys. Rev.* A **46** (1992): R2992.
2. Bohr, T., Pedersen, A. W., and M. H. Jensen. *Phys. Rev.* A **42** (1990): 3626.
3. Bohr, T., Pedersen, A. W., Jensen, M. H., and D. A. Rand. In *New Trends in Nonlinear Dynamics and Pattern Forming Phenomena: The Geometry of Nonequilibrium*, edited by P. Coullet and P. Huerre. New York: Plenum, 1989.
4. Geil, P. H. *Polymer Single Crystals.* New York: Interscience, 1963.
5. Gil, L., Lega, J., and J. L. Meunier. *Phys. Rev.* A **41** (1990): 1138.
6. Huber, G., and P. Alstrøm. *Physica* A **195** (1993): 448.
7. Huber, G., Alstrøm, P., and T. Bohr. *Phys. Rev. Lett.* **69** (1992): 2380.
8. Keller, A. In *Polymers, Liquid Crystals, and Low-Dimensional Solids*, edited by N. March and M. Tosi. New York: Plenum, 1984.
9. Kuramoto, Y. *Chemical Oscillations, Waves, and Turbulence* Berlin: Springer, 1984.
10. Newell, A. C., and J. A. Whitehead. *J. Fluid Mech.* **38** (1969): 279.
11. Oono, Y., and S. Puri. *Phys. Rev. Lett.* **58** (1987): 836.
12. "Zamboni" is the name popularly given (in the USA) the large machines that sweep and level the ice during the intermissions of hockey games. Since the machines render the rink's disordered surface smooth, and do so in a spiral pattern, it is an oddly appropriate image in the context of nucleating spiral-wave droplets.

FIGURE CAPTIONS

Figure 1: Phase diagram for $0 \leq \alpha \leq 2$ and $-2 \leq \beta \leq 0$. Curves are labeled (BF) Benjamin-Feir, (T) turbulence transition, (NUC) nucleation limit, (ECK) Eckhaus instability.

Figure 2: Decay of vortex density in time, from random initial conditions, for $\alpha = 0.75, \beta = -1$, lattice size 512×512. Four dynamical regimes are indicated.

Figure 3: Nucleation sequence. Dark points are vortices (amplitude minima), dark lines are domain walls (amplitude maxima). $\alpha = 0.79, \beta = -1$, 1024×1024 lattice. (a) Early, (b) intermediate and (c) late stages.

Figure 4: Vortex density vs. time for the "Zamboni" clean-up, i.e. fast decay to the frozen state. Two parameter values, $\beta = -1$ for both. Curves are best quadratic fits.

Figure 5: Domain walls are nearly hyperbolic, since the path difference $r_1 - r_2$ between two frozen vortices is a constant, being proportional to the time interval between their times of nucleation.

Figure 6: Polycrystalline structures. (a) Grains of polycrystalline alumina (MgO doped and hot pressed). (Courtesy of A. M. Glaeser and J. Rödel.) (b) Spherulites (5 cells) of polyethylene crystallized from the melt, as observed between crossed polarizers. Horizontal scale of the photograph is 130 μm. (Courtesy of P. H. Geil.)

Figure 7: Schematic of a negatively-charged braid. Circles represent vortices, lines represent domain walls.

Figure 8: Amplitude isosurfaces in a three-dimensional CGL simulation. Tubes are low-amplitude surfaces around vortex filaments; sheets are high-amplitude surfaces bordering domain walls. A two-dimensional slice with amplitude shading is also shown.

Figure 1

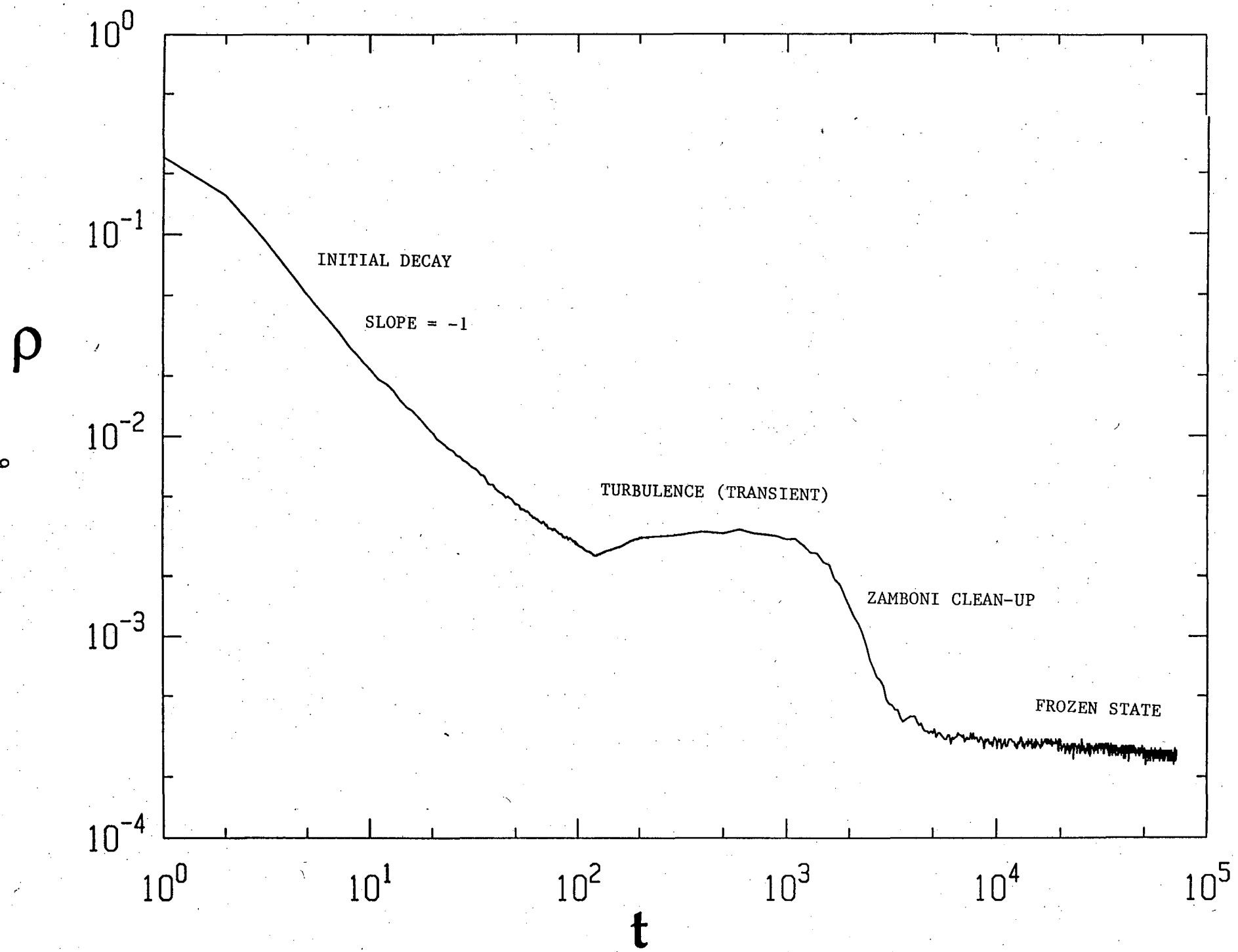
10^0
10^{-1}
10^{-2}
10^{-3}
10^{-4}
ρ
INITIAL DECAY
SLOPE = -1
TURBULENCE (TRANSIENT)
ZAMBONI CLEAN-UP
FROZEN STATE
10^0
10^1
10^2
10^3
10^4
10^5
t

Figure 2

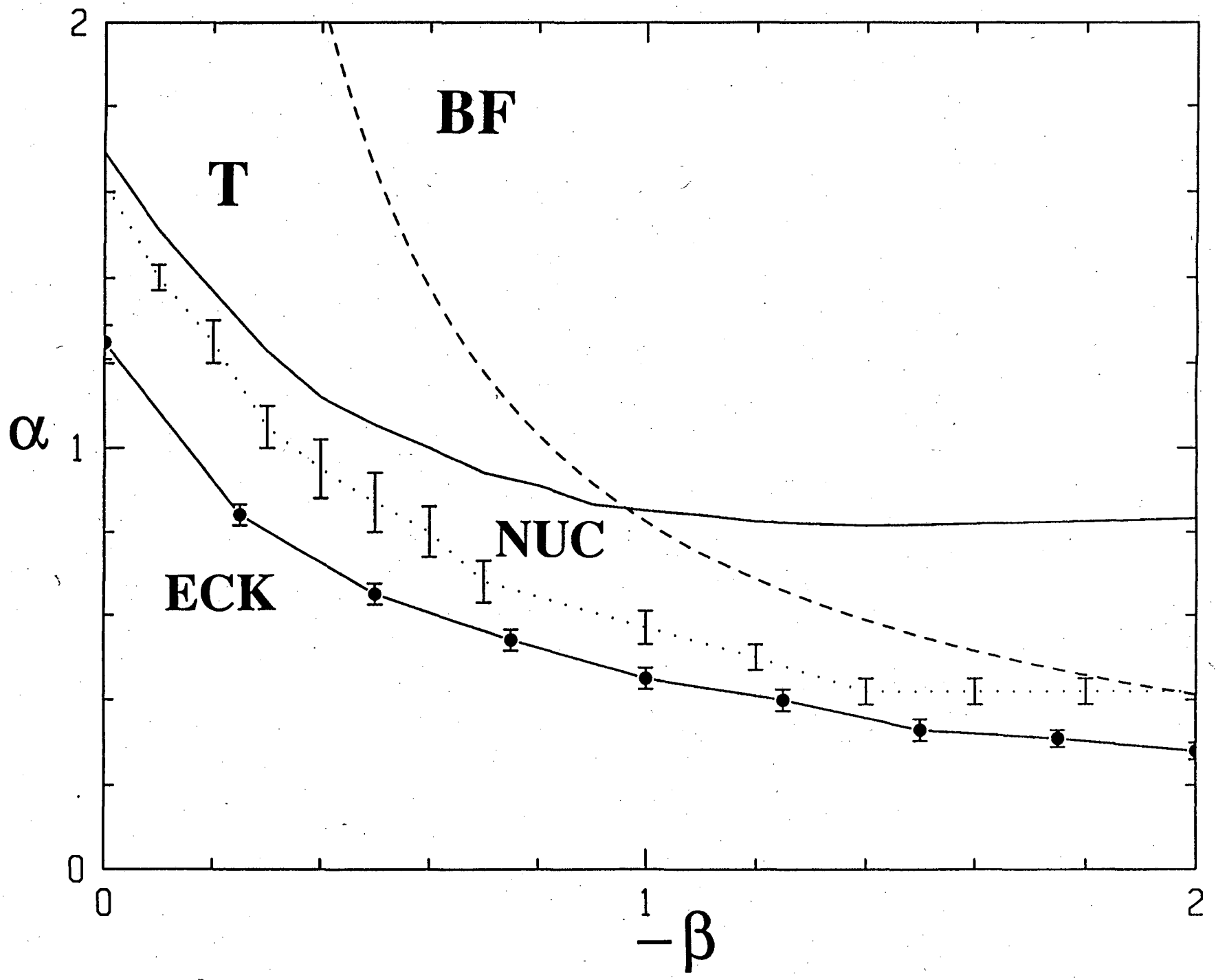

Figure 3 (a)

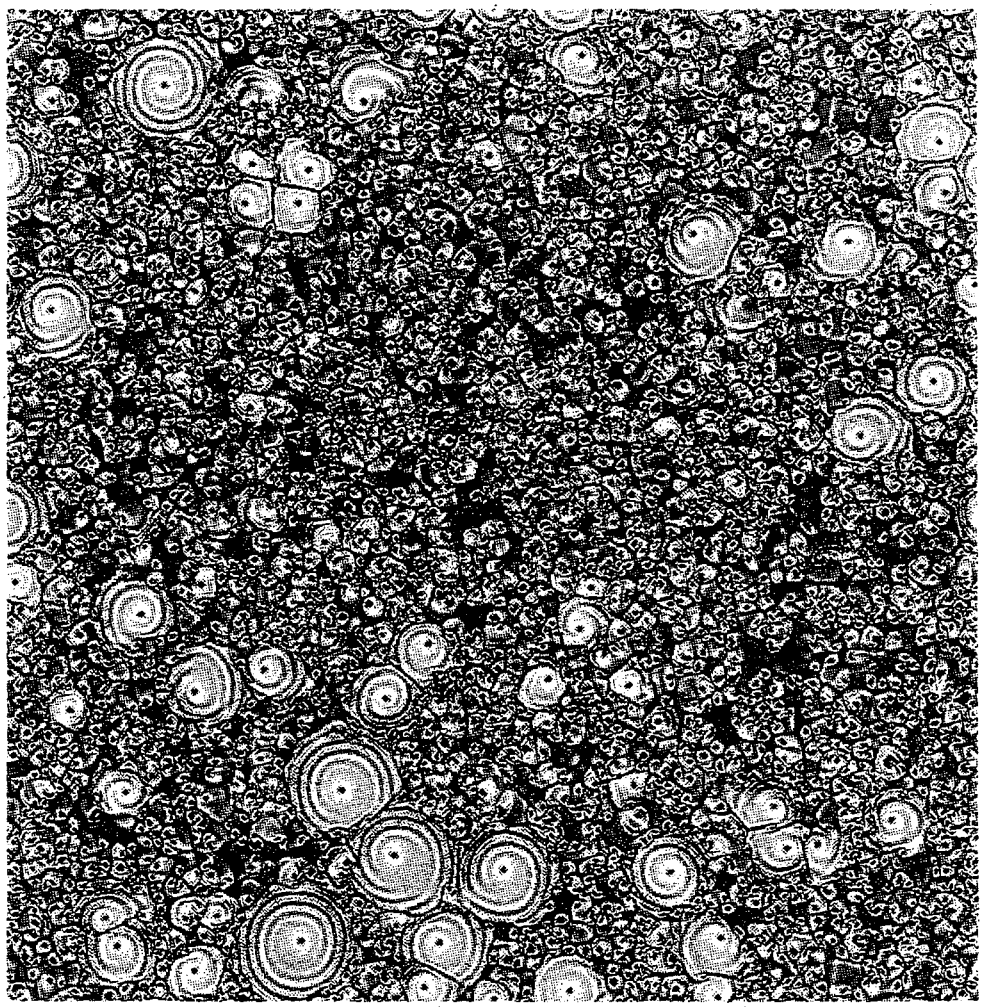

Figure 3 (b)

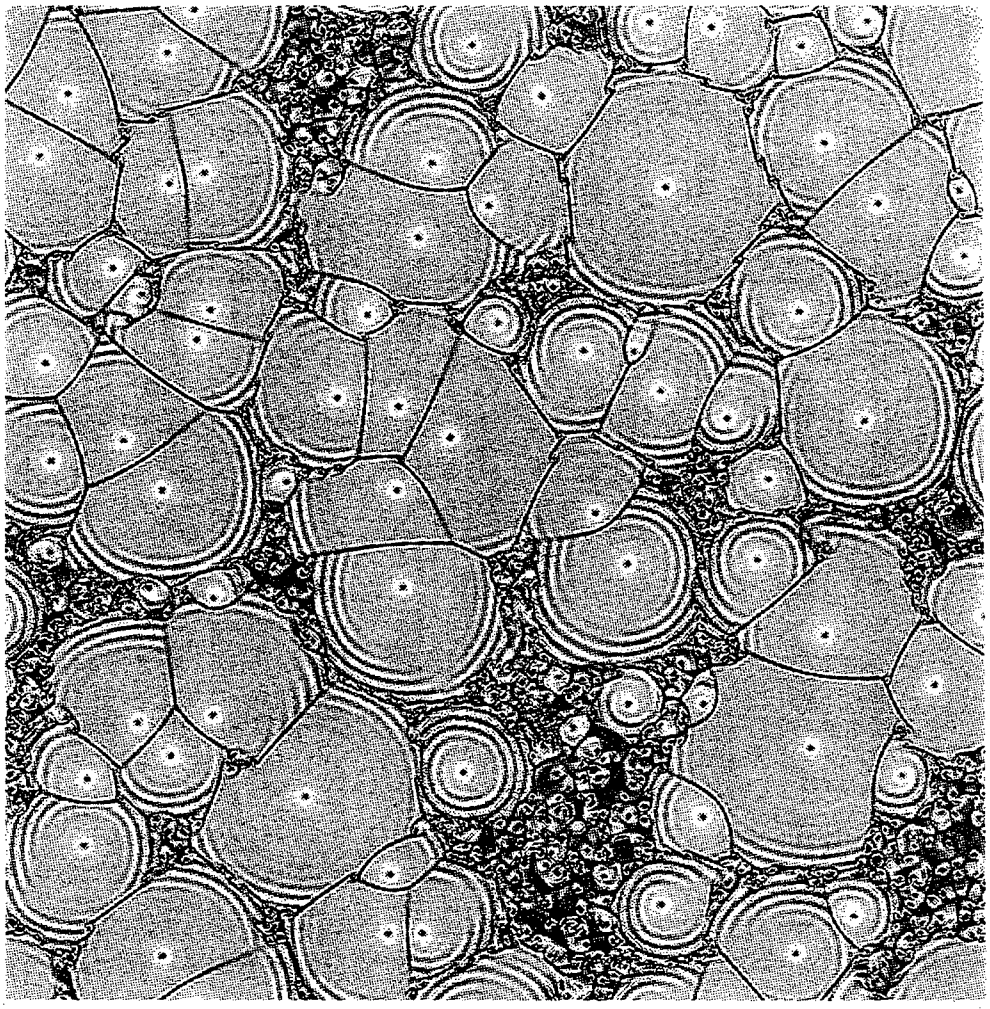

Figure 3 (c)

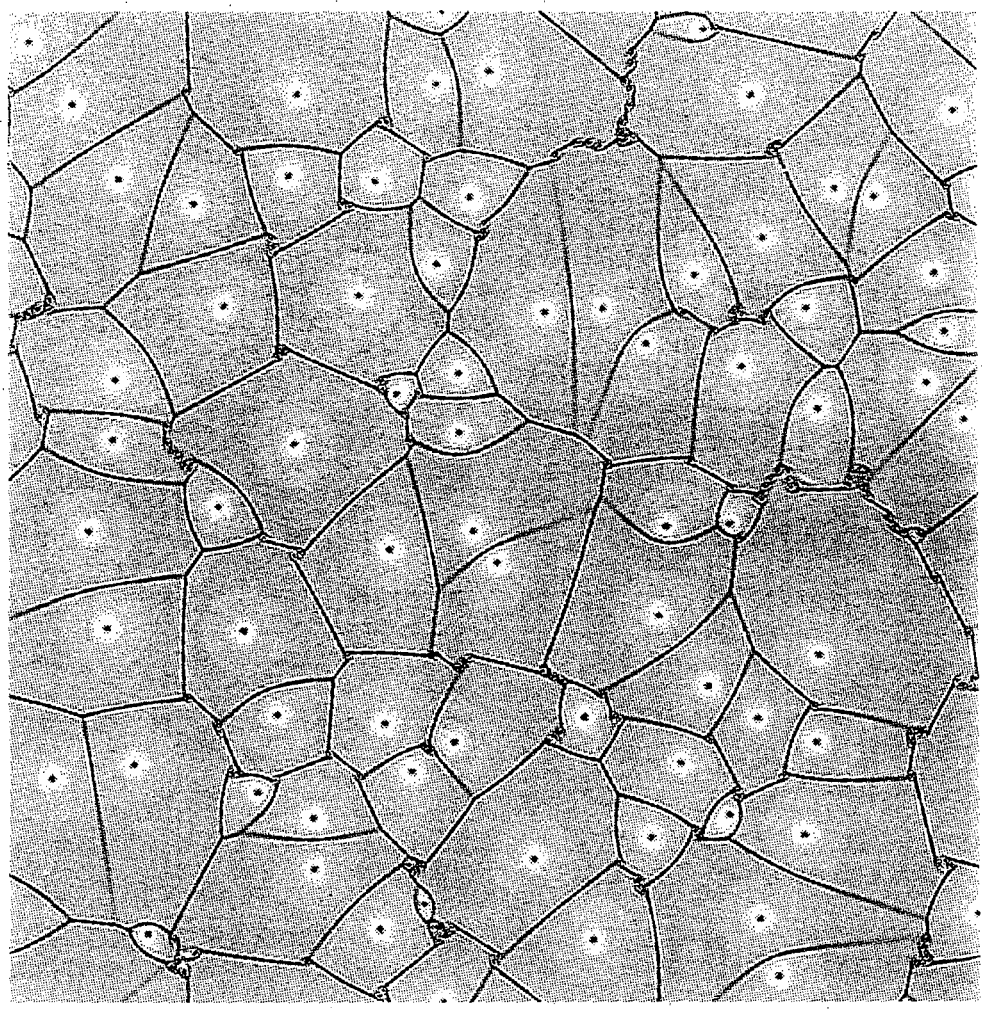

Figure 4

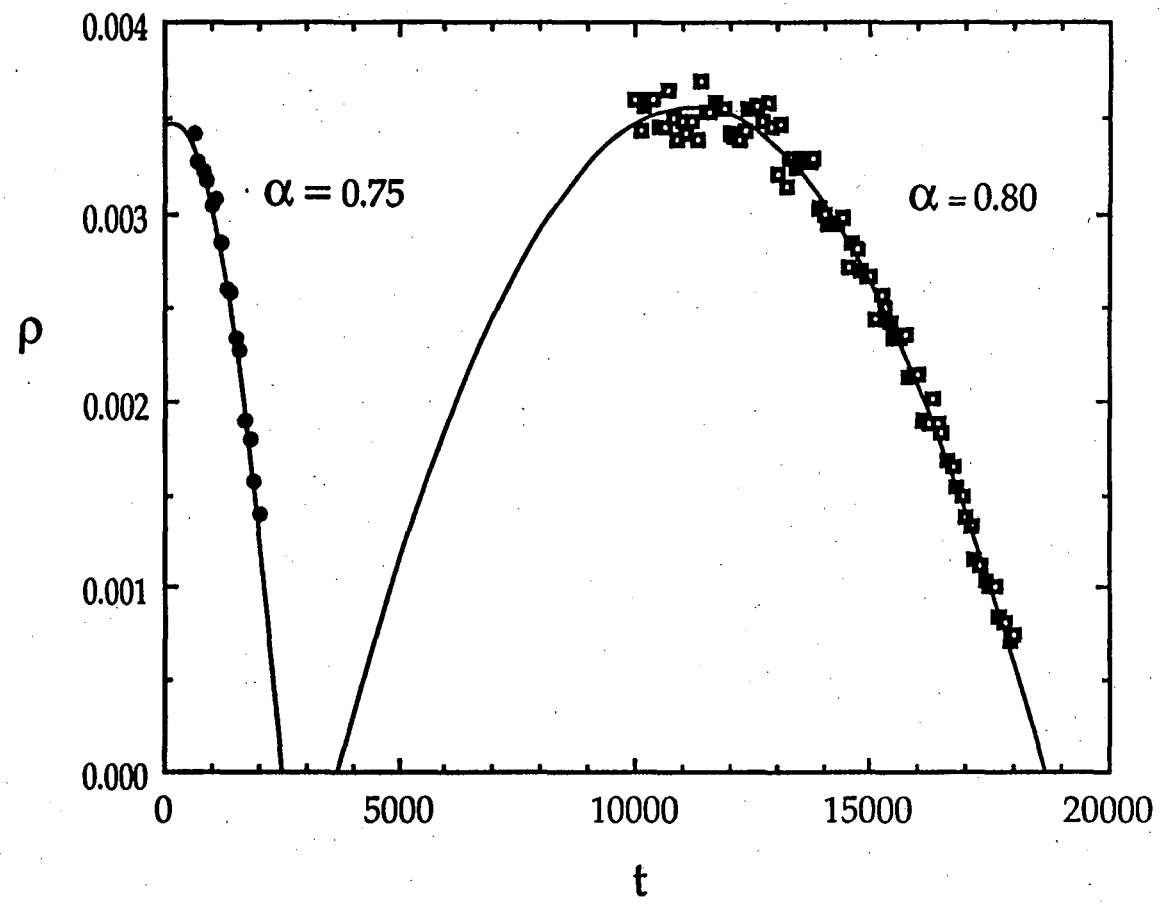
0.004
0.003
0.002
0.001
0.000
ρ
α = 0.75
α = 0.80
0
5000
10000
15000
20000
t

Figure 5

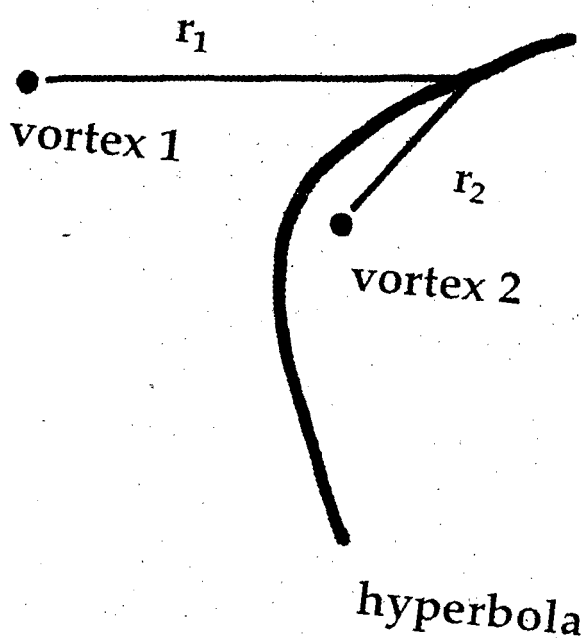

Figure 6 (a)

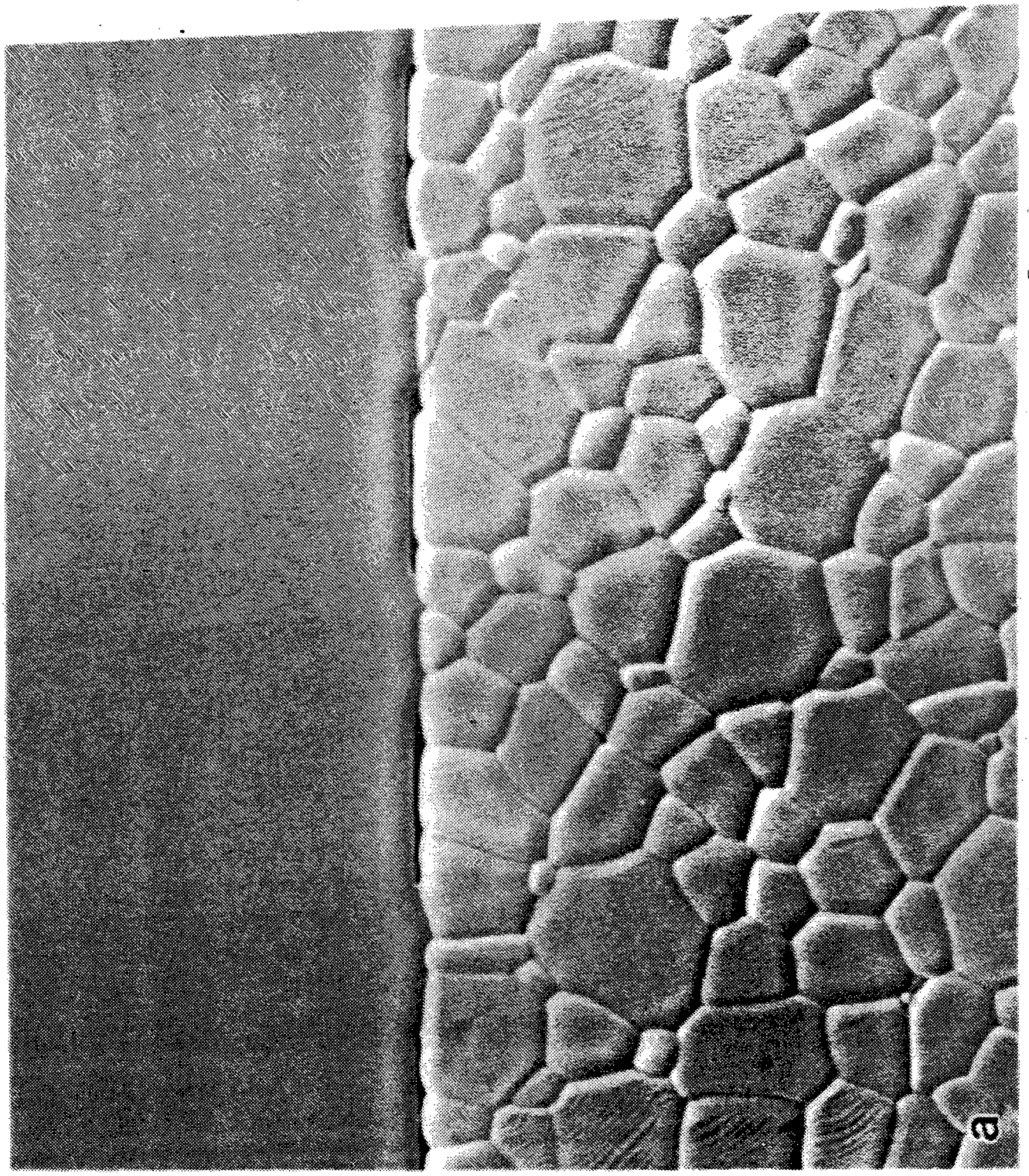

Figure 6 (b)

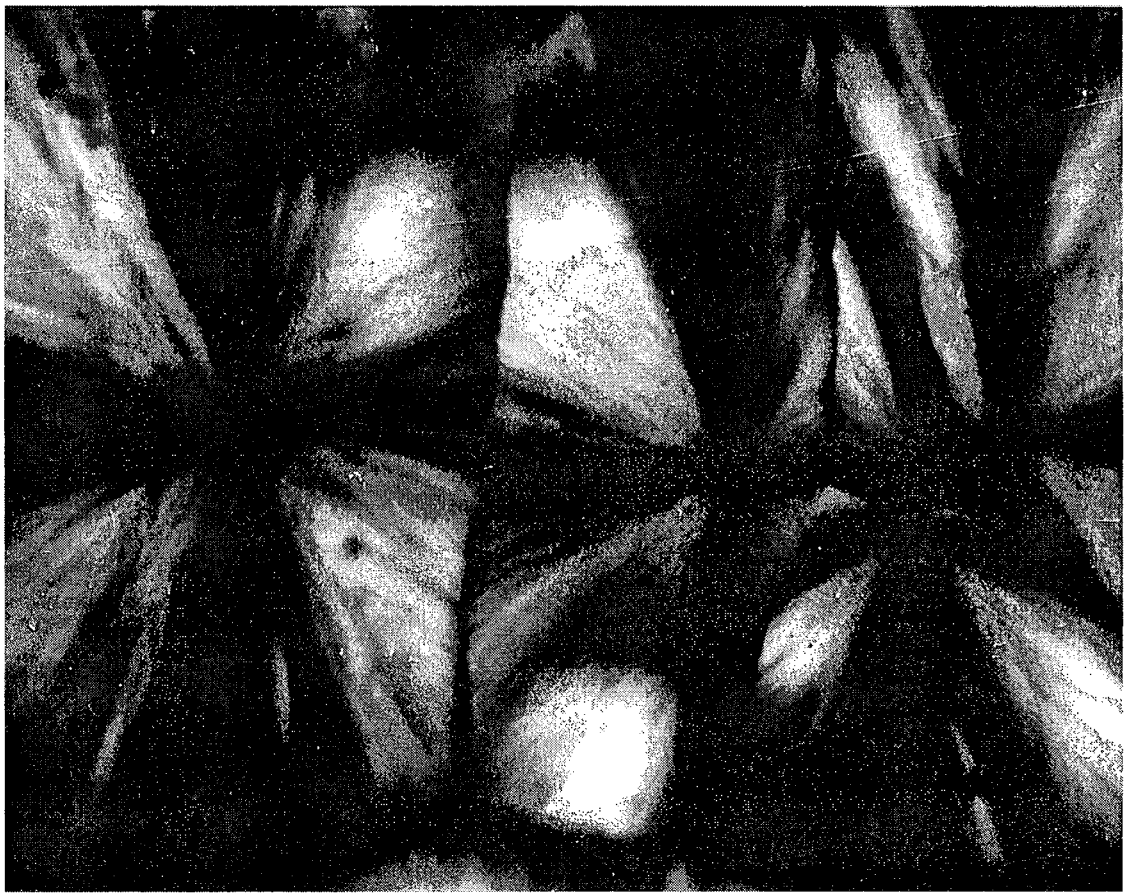

b

Figure 7

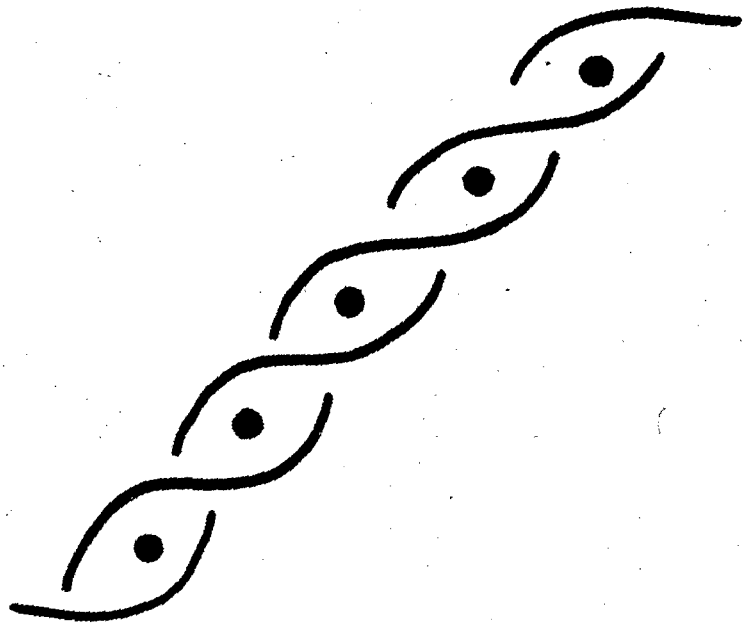

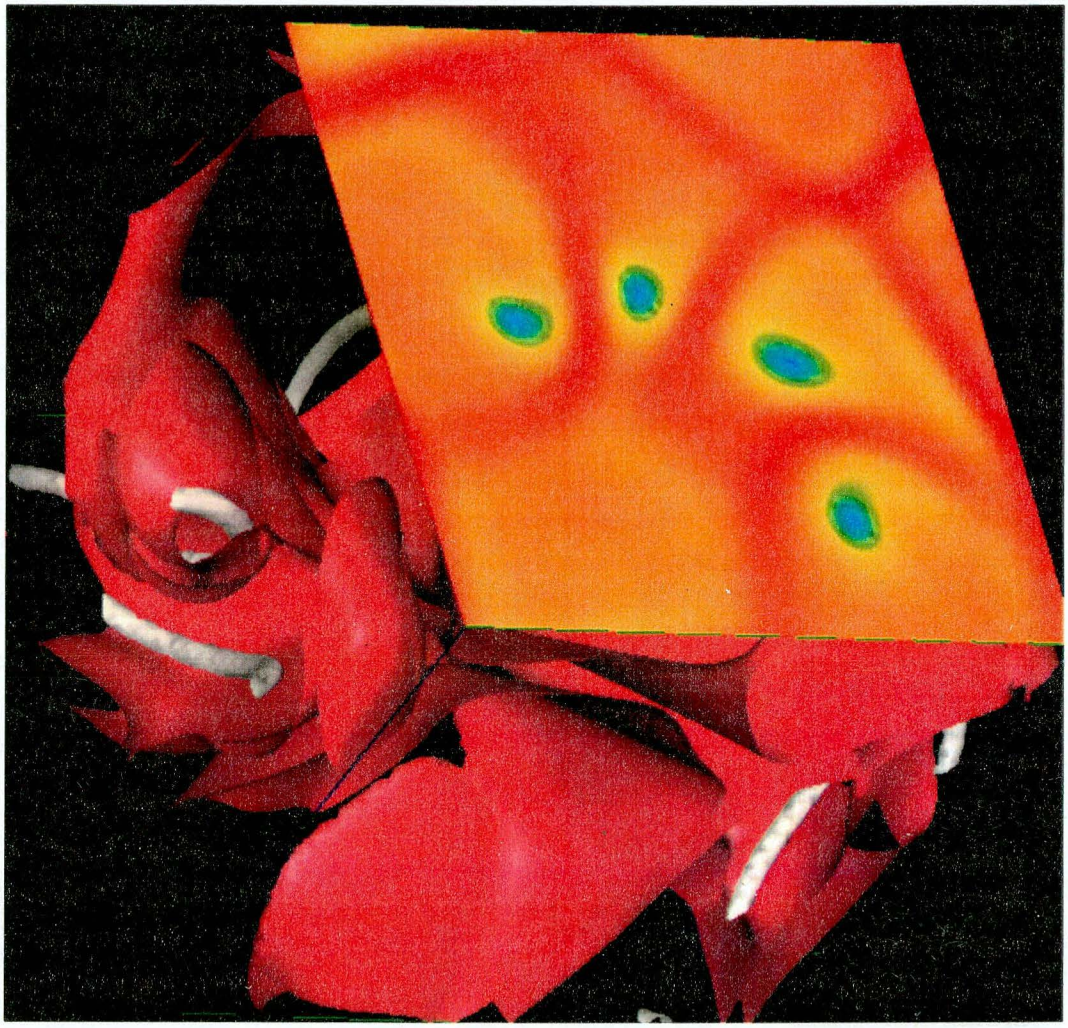

Figure 8

LAWRENCE BERKELEY LABORATORY
UNIVERSITY OF CALIFORNIA
TECHNICAL INFORMATION DEPARTMENT
BERKELEY, CALIFORNIA 94720